Dynamics of the sub-Ohmic spin-boson model: A comparison of three numerical approaches

Yao Yao,[1,2] Liwei Duan,[1] Zhiguo Lü,[3] Chang-Qin Wu,[2] and Yang Zhao[1,*]

[1]*Division of Materials Science, Nanyang Technological University, 50 Nanyang Avenue, Singapore 639798*

[2]*State Key Laboratory of Surface Physics and Department of Physics, Fudan University, Shanghai 200433, China*

[3]*Key Laboratory of Artificial Structures and Quantum Control, and Department of Physics, Shanghai Jiao Tong University, Shanghai 200240, China*

(Received 27 May 2013; revised manuscript received 15 July 2013; published 16 August 2013)

Dynamics of the sub-Ohmic spin-boson model is examined using three numerical approaches, namely the Dirac-Frenkel time-dependent variation with the Davydov D_1 ansatz, the adaptive time-dependent density matrix renormalization group method within the representation of orthogonal polynomials, and a perturbative approach based on a unitary transformation. In order to probe the validity regimes of the three approaches, we study the dynamics of a qubit coupled to a bosonic bath with and without a local field. Comparison of the up-state population evolution shows that the three approaches are in agreement in the weak-coupling regime but exhibit marked differences when the coupling strength is large. The Davydov D_1 ansatz and the time-dependent density matrix renormalization group can both be reliably employed in the weak-coupling regime, while the former is also valid in the strong-coupling regime as judged by how faithfully the trial state follows the Schrödinger equation. We further explore the bipartite entanglement dynamics between two qubits coupled with individual bosonic baths which reveals entanglement sudden death and revival.

DOI: 10.1103/PhysRevE.88.023303 PACS number(s): 05.10.−a, 05.30.Jp, 03.65.Yz, 75.40.Mg

I. INTRODUCTION

Environment-induced dissipation, including phase and population damping, plays a central role in ultrafast energy transfer in optoelectronic processes [1–4], quantum simulation with trapped ions and superconducting qubits [5,6], and quantum information processing in noisy channels [7–10]. Recently, it has been speculated that the high efficiency of excitation energy transfer in green sulfur bacteria is attributed to the long-lived coherence uncovered in the Fenna-Matthew-Olson complex [11,12]. A number of factors are to blame for the loss of coherence in a quantum system, including finite temperature, energetic disorder, and dynamic disorder. Dynamic disorder [13], also known as electron-phonon or exciton-phonon coupling, adds flavor to the decoherence process and is recognized as a key factor in excitation energy transfer. Models of system-environmental coupling [3], such as the spin-boson model, are often employed to help uncover environment-induced mechanisms of decoherence. A related effect of interest is entanglement sudden death and revival arising from finite-temperature decoherence [7,14], for which a comprehensive understanding is still elusive due to a lack of an accurate theory. A dimer structure, which contains a two-qubit system coupled with individual bosonic baths, such as two spin-boson models with correlated spin initial states and interspin coupling, can be helpful in finding answers to the problem of entanglement death and revival and resolving issues such as competition between hopping and recombination, the environment-induced superselection, and the entanglement dynamics.

Despite sustained interest in the spin-boson model [15,16] that spans several decades, this simple system of a spin coupled to a bath of bosons still occupies a central place in a variety of fields, ranging from excitation energy transport in molecular [2,3] and natural photosynthetic systems [4] to quantum entanglement and computation [8,9]. One focus of those studies is the coherent-incoherent transition in various parameter regimes. Whether a localized state exists in the sub-Ohmic regime has been, in particular, an issue of intense contention in the community [17–26]. Using the polaron ansatz, Chin *et al*. studied the continuous transition in the deep sub-Ohmic regime. They found an obvious cusp in both the spin coherence and the spin-boson entanglement at the critical point. The cusps are explained by the differing mechanisms via which the spin coherence is modified by the fast adiabatic modes and the slow nonadiabatic modes of the bath. In addition, a similar ansatz is also adopted by the numerical renormalization group (NRG) method to study the phase transition in the same regime. With regard to spin-boson dynamics, decoherence and relaxation in the sub-Ohmic regime, where medium to strong system-environment coupling exists, are of great relevance to many practical problems, and, therefore, much theoretical attention has been devoted to the sub-Ohmic model, resulting in a large body of varying results that beg for comparison. The list includes, but is not limited to the following: the numerically exact real-time path integral method with quasiadiabatic propagator revealing effective dynamic asymmetry in the presence of a sub-Ohmic bath [26,27]; the quantum Monte Carlo method, which determines the critical exponents for an s value less than a half [28]; the NRG method developed by Wilson [29], which reveals a continuous quantum phase transition in the sub-Ohmic regime and weakly damped coherent oscillations on short time scales in the localized phase [30]; the numerically exact multilayer multiconfiguration time-dependent Hartree method (ML-MCTDH) uncovering the transition of the dynamics from weakly damped coherent motion to localization on increase of the system-bath coupling strength [19]; the sparse polynomial

*Author to whom correspondence should be addressed: yzhao@ntu.edu.sg

representation method based on exact diagonalization [31]; and the real-time path integral Monte Carlo techniques, which show that the coherent phase exists even under strong dissipation for $s < 1/2$ [17,18].

The spin-bath interactions are formally identical to the exciton-phonon coupling in the Holstein molecular crystal model [32–34], for which a hierarchy of trial states based on the Davydov ansätze has been widely used for describing the exciton-phonon dynamics. As a semiclassical approach for studying energy transport in deformable molecular chains, those ansätze [35] were put forward by Davydov and coworkers. It was pointed out later [36] that the Davydov ansatz bears close resemblance to a multiconfigurational ansatz with more than one Slater determinant. By exploiting the analogy between the spin-boson model and the Holstein molecular crystal model, a time-dependent trial wave function very similar to the Davydov D_1 ansatz is proposed to provide an accurate, yet efficient, description for dynamical properties of the sub-Ohmic spin-boson model.

Given difficulties in solving the sub-Ohmic spin-boson model exactly, a few suitable approximation schemes are invariably required for comparisons. The NRG method is among the early approaches applied to the spin-boson model via a mapping that relies on a logarithmic discretization in the frequency domain [37], and it was found that there exists a localized state in the strong-coupling regime where the coherence is suppressed. The density matrix renormalization group (DMRG) algorithm [38], which is robust in dealing with one-dimensional lattice with only nearest-neighbor interactions, was subsequently applied to study this model. Using the theory of orthogonal polynomials, several discretization schemes were proposed for incorporation in the DMRG method [39]. Subsequently, using the adaptive time-dependent DMRG (t-DMRG) method [40], a molecular dimer coupled to two individual baths was studied [41]. On the other hand, the exactly solvable Landau-Zener Hamiltonian closely related to the spin-boson model has been investigated comprehensively using the t-DMRG approach [42]. The latter work mainly examined the precision of the numerical calculation, especially for the linear and logarithmic discretizations, and it was found that the t-DMRG method works well for the spin-boson model when the time scale is not too long but still within the practice purposes.

In this paper, an approach based on a unitary transformation, one that is at variance with the usual unitary transformation methods in the literature [43], is applied to study the nonadiabatic correlations between the spin and bosons in the spin-boson model [44]. In the traditional theory of unitary transformation which gives valid results in the scaling limit, the expansion parameter is the tunneling integral, while in the unitary transformation used in this work it is a momentum-dependent variable, and many important results have been obtained on the quantum phase transition and the coherence-incoherence crossover for the sub-Ohmic and Ohmic baths. Using our transformation, we have also carried out checks on the Shiba relation and the sum rules in a broad parameter space including the scaling limit. In this work, results from this approach will be compared with those from the Davydov ansatz and the t-DMRG method.

This paper is organized as follows. The Davydov D_1 ansatz, the t-DMRG algorithm, and a perturbative approach with unitary transformation for the spin-boson model are introduced in Sec. II. Calculation results for one qubit will be presented in Sec. III, where the comparisons between different theories for population evolution are shown. Discussions on the extent of validity for different theories are also presented. The dynamical behavior of the two qubits as well as the evolution of entanglement is discussed in the fourth section. Conclusions are drawn in the final section.

II. METHODOLOGIES

A. Davydov D_1 ansatz

The Hamiltonian of the spin-boson model is typically written as

$$H = \frac{\epsilon}{2}\sigma^z - \frac{\Delta}{2}\sigma^x + \sum_l \omega_l b_l^\dagger b_l + \frac{\sigma^z}{2}\sum_l \lambda_l (b_l^\dagger + b_l), \quad (1)$$

where $\hbar$ is set to unity, σ^z and σ^x are the usual Pauli operators, ϵ is the spin bias due to the influence of a local field, Δ is the tunneling constant, ω_l is the frequency of the l-th boson mode, $b_l^\dagger (b_l)$ are the creation (annihilation) operators of the l-th mode, and λ_l labels the coupling strength of the spin to the boson of l-th mode. There is a cutoff frequency for the bosons at ω_c so the spectral function is expressed as $J(\omega) = 2\pi\alpha\omega_c^{1-s}\omega^s e^{-\omega/\omega_c}$. For the sake of simplicity in numerical computations, ω_c is set to be 1. The sub-Ohmic bosonic regime, corresponding to $s < 1$, is of particular theoretical interest, as the quantum phase transition between the localized and delocalized phases has been studied by a number of approaches. In this work, the sub-Ohmic bath ($s = 1/4$) is considered.

As a trial wave function used in the variational algorithm, the Davydov D_1 ansatz is composed of a linear superposition of coherent states [45]

$$|D_1(t)\rangle = \sum_n A_n(t)|n\rangle \otimes \exp\left[\sum_l B_{n,l}(t) b_l^\dagger - B_{n,l}^*(t) b_l\right] |0\rangle_b, \quad (2)$$

where $A_n(t)$ and $B_{n,l}(t)$ are variational parameters for the spin and boson parts of the binary system, respectively, n takes two values, $+$ and $-$, to denote the up and down spin states, respectively, and $|0\rangle_b$ is the bosonic vacuum state. The main step of our procedure is to project the state

$$|\delta D(t)\rangle = \left(i\frac{\partial}{\partial t} - H\right)|D_1(t)\rangle \quad (3)$$

onto the states $|n\rangle \otimes U_n^\dagger|0\rangle_b$ and $|n\rangle \otimes U_n^\dagger b_l^\dagger|0\rangle_b$, where $U_n^\dagger \equiv \exp[\sum_l B_{n,l}(t) b_l^\dagger - B_{n,l}^*(t) b_l]$. It should be noted that this projection procedure is equivalent to the Lagrangian formalism [45–47] of the Dirac-Frenkel time-dependent variation used in Ref. [48]. The equation of motion for $A_n(t)$ can be written as

$$\begin{aligned} -i\frac{\partial}{\partial t}A_\pm(t) = A_\pm(t)\sum_l \Bigg[\frac{i}{2}\left(B_{\pm,l}^*(t)\frac{\partial}{\partial t}B_{\pm,l}(t) - \text{c.c.}\right) \\ - \omega_l |B_{\pm,l}(t)|^2 \mp \frac{\lambda_l}{2}(B_{\pm,l}(t) + \text{c.c.})\Bigg] \\ \mp \epsilon/2 A_\pm(t) + \frac{\Delta}{2}A_\mp(t) S_{\pm,\mp}, \end{aligned} \quad (4)$$

where $\pm$ denotes spin-up (+) and -down (−) and $S_{n,n'} \equiv {}_b\langle 0|U_n U_{n'}^\dagger|0\rangle_b$. Similarly, for $B_{n,l}(t)$, the equation of motion can be written as

$$-iA_\pm(t)\frac{\partial}{\partial t}B_{\pm,l}(t) = -\omega_l A_\pm(t)B_{\pm,l}(t) \mp \frac{\lambda_l}{2}A_\pm(t) + \frac{\Delta}{2}A_\mp(t)S_{\pm,\mp}(B_{\mp,l} - B_{\pm,l}). \quad (5)$$

Using the Dirac-Frenkel variational principle, the sub-Ohmic spin-boson model has been recently studied, confirming that a persistent population oscillation still exists in the presence of a very large coupling strength for $s < 1/2$ when the polarized initial condition is used [48]. It is intriguing that the polarized bath initial condition is more likely to lead to coherent dynamical behaviors than the factorized initial condition, which indicates that the dynamics of the sub-Ohmic spin-boson model is rather sensitive to the choice of initial conditions. Evidence was also presented to show that the variational approach based on the Davydov D_1 ansatz is robust in the strong-coupling regime, where the boson component of the time-dependent wave function is better captured by a superposition of coherent states. Similar trends were also observed in the application of the Davydov D_1 ansatz to the Holstein molecular crystal model [49,50]. However, as the sub-Ohmic bath implies relatively strong spin-boson interactions, the validity range of the D_1 ansatz can be extended to moderate and weak coupling in the presence of the sub-Ohmic bath, a fact that will be shown by the comparisons with other numerical methods.

B. Adaptive time-dependent density matrix renormalization group

In this subsection, we give a brief description of implementing the t-DMRG method to the spin-boson model. The DMRG method is a powerful numerical technique to treat one-dimensional systems with short-ranged interactions. In order to extend it to study the time evolution, one needs to truncate the Hamiltonian into the summation of terms with only nearest-neighbor interactions, such as $H = \sum_j H_j$ with H_j being the Hamiltonian of the jth bond. The Trotter decomposition of the evolution operator, in the form of

$$e^{iH\tau} \simeq \prod_j e^{iH_j\tau}, \quad (6)$$

can then be applied to the DMRG-computed states. Herein, τ should be kept small to put a lip on the error of the decomposition, and, depending on the required precision, decompositions of various orders can be selected. Throughout this work, we use the second-order Trotter decomposition.

As the purpose of the decomposition is to transform the Hamiltonian to a DMRG-friendly form, it is necessary to map the bosonic modes onto a one-dimensional chain with only nearest-neighbor hopping. To this end, one can perform either a linear discretization scheme or a logarithmic one for the bosons prior to the transformation. These two discretization schemes have been carefully compared for t-DMRG [42]. In this work we will utilize logarithmic discretization and follow the theory of orthogonal polynomials [41], which yields good accuracy if the total number of discretized modes is not very large. The final transformed Hamiltonian has the form

$$\tilde{H} = H_s + \sqrt{\frac{\eta}{4\pi}}\sigma^z(b_0^\dagger + b_0) + \sum_i \omega_i b_i^\dagger b_i + \sum_i (t_i b_{i+1}^\dagger b_i + \text{H.c.}), \quad (7)$$

where H_s labels the spin Hamiltonian to be discussed later, ω_i and t_i are the transformed frequency and hopping integral of bosons [41], respectively, η is the renormalized spin-boson coupling, which could be estimated from $\eta = \int_0^{\omega_c} J(\omega)d\omega$. Results from the logarithmic discretization procedure with the discretization parameter Γ can be written as

$$\omega_i = \xi_s(P_i + Q_i), \quad (8)$$

$$t_i = -\xi_s P_i\left(\frac{N_{i+1}}{N_i}\right), \quad (9)$$

with

$$\xi_s = \frac{(s+1)[1-\Gamma^{-(s+2)}]}{(s+2)[1-\Gamma^{-(s+1)}]}\omega_c, \quad (10)$$

$$P_i = \frac{\Gamma^{-i}(1-\Gamma^{-(j+s+1)})^2}{[1-\Gamma^{-(2i+s+1)}][1-\Gamma^{-(2i+s+2)}]}, \quad (11)$$

$$Q_i = \frac{\Gamma^{-(i+s)}(1-\Gamma^{-j})^2}{[1-\Gamma^{-(2i+s)}][1-\Gamma^{-(2i+s+1)}]}, \quad (12)$$

$$N_i^2 = \frac{\Gamma^{-i(s+1)}(\Gamma^{-1};\Gamma^{-1})_i^2}{[\Gamma^{-(s+1)};\Gamma^{-1}]_i^2[1-\Gamma^{-(2i+s+1)}]}, \quad (13)$$

where

$$[a;q]_i = (1-a)(1-aq)\cdots(1-aq^{i-1}). \quad (14)$$

We have checked the dependence of our results on the number of bosons in each mode (ranging from 4 to 8). In the weak-coupling regime, the results show good convergence with 4 bosons, while in the strong-coupling regime, even a boson number of 8 is sometimes insufficient, which is why we conclude that the DMRG is more efficient for weak coupling. On the other hand, a smaller boson number brings a higher computational efficiency. Considering these two aspects, a boson number from 4 to 8 is used in this work.

In order to improve the numerical accuracy, two issues need to be addressed. First, the spin Hamiltonian H_s can be written as

$$H_s = \sum_l \frac{\epsilon_l}{2}\sigma_l^z - \sum_l \frac{\Delta}{2}\sigma_l^x + J\sigma_1\cdot\sigma_2, \quad (15)$$

which has a DRMG-friendly dimer structure with two coupled spin-boson Hamiltonians that will be used throughout this work. Here l is the spin index, ϵ_l the local magnetic field, and J the exchange constant. The spins are located at the center of the chain where the numerical precision is the highest. For the purpose of discussing one spin case, we set $J = 0$, and spin dynamics under the competition between J and Δ will be investigated later. Instead of the usual polarized or factorized bath initial states chosen for the spin-boson model, the ground state of the Hamiltonian (7) with a large bias is chosen as the initial state, that is, ϵ_l is given relatively large positive (negative) values for spin-down (spin-up) state.

During time evolution, ϵ_l will be gradually decreased until a specific chosen value is reached. This treatment should be much more accurate than one in which the bias is suddenly switched on and off, since the optimized basis for t-DMRG cannot undergo sudden changes during the initial period of the evolution. In all our calculations, the DMRG truncation number is 100, the discretization parameter $\Gamma = 1.5$, and the number of sites in the chain is around 100 depending on the model parameters.

C. Perturbation theory with unitary transformation

We also present an analytical treatment based on the unitary transformation approach [44,51]. A canonical transformation is applied to the Hamiltonian, i.e., $H' = \exp(S)H\exp(-S)$, with the generator S defined as

$$S = \sum_k \frac{g_k}{2\omega_k}(b_k^\dagger - b_k)[\xi_k\sigma^z + (1-\xi_k)\sigma_0\mathbf{I}]. \tag{16}$$

Here σ_0 is a constant, $\mathbf{I}$ is the identity matrix, and ξ_k are k-dependent functions given in Ref. [44]. After performing the transformation, one obtains the expression for the transformed Hamiltonian H':

$$\begin{aligned}
H' &= H_0' + H_1' + H_2',\\
H_0' &= -\frac{1}{2}\Delta_r\sigma^x + \frac{1}{2}\epsilon'\sigma^z + \sum_k \omega_k b_k^\dagger b_k\\
&\quad - \sum_k \frac{g_k^2}{4\omega_k}\xi_k(2-\xi_k) + \sum_k \frac{g_k^2}{4\omega_k}\sigma_0^2(1-\xi_k)^2, \qquad (17)\\
H_1' &= \frac{1}{2}\sum_k g_k(1-\xi_k)(b_k^\dagger + b_k)(\sigma^z - \sigma_0) - \frac{1}{2}\Delta_r i\sigma^y B,\\
H_2' &= -\frac{1}{2}\Delta\sigma^x(\cosh\{B\} - \eta) - \frac{1}{2}\Delta i\sigma^y(\sinh\{B\} - \eta B),
\end{aligned}$$

where H_0' is the unperturbed part of H', H_1' denotes the first-order terms where all the higher-order terms are included in H_2' [44], $B = \sum_k \frac{g_k}{\omega_k}\xi_k(b_k^\dagger - b_k)$, and the renormalized tunneling integral $\Delta_r = \eta\Delta$ with η determined by $\langle\cosh\{B\}\rangle = \eta$ (thermally averaged with respect to the Bose-Einstein distribution) as follows:

$$\eta = \exp\left[-\sum_k \frac{g_k^2}{2\omega_k^2}\xi_k^2\right], \quad 0 \leqslant \eta \leqslant 1. \tag{18}$$

The shifted bias is renormalized as

$$\epsilon' = \epsilon - \tau\sigma_0, \quad \tau = \sum_k \frac{g_k^2}{\omega_k}(1-\xi_k)^2. \tag{19}$$

H_0', which can be solved exactly because the spin and bosons in H_0' are decoupled, is diagonalized by a unitary matrix $U = u\sigma^z + v\sigma^x$, where $u = \sqrt{(1-\frac{\epsilon'}{W})/2}$, $v = \sqrt{(1+\frac{\epsilon'}{W})/2}$, and $W = \sqrt{\epsilon'^2 + \Delta_r^2}$. Thus, $\tilde{H}_0 = U^\dagger H_0 U = -\frac{1}{2}W\sigma^z + \sum_k \omega_k b_k^\dagger b_k - \sum_k \frac{g_k^2}{4\omega_k}\xi_k(2-\xi_k) + \sum_k \frac{g_k^2}{4\omega_k}\sigma_0^2(1-\xi_k)^2$, and we obtain the ground state $|g_0\rangle$ with energy E_g. Further, $\tilde{H}_1 + \tilde{H}_2 = U^\dagger(H_1' + H_2')U$ are treated as perturbation which should be kept as small as possible. For this purpose ξ_k is properly determined. Note that $\tilde{H}_1|g_0\rangle = 0$ and this is the key point in the unitary transformation approach. Thus, the ground-state energy E_g agrees well with those of the NRG in both the zero-bias and finite-bias cases [44]. The original Hamiltonian can be solved exactly in two limits: (1) the weak-coupling limit $\alpha \to 0$ with $E_g(\alpha \to 0) = -\frac{1}{2}\sqrt{\Delta^2 + \epsilon^2}$ and (2) the zero tunneling limit $\Delta \to 0$ with $E_g(\Delta \to 0) = -\frac{1}{2}|\epsilon| - \sum_k \lambda_k^2/4\omega_k$. It is easily checked that E_g goes to the correct ground-state energy in the two limits.

In the dynamics calculation, the transformed Hamiltonian is approximated as $\tilde{H} \approx \tilde{H}_0 + \tilde{H}_1$, since the terms in $\tilde{H}_2$, such as $b_k b_{k'}$ and $b_k^\dagger b_{k'}^\dagger$, are related to the multiboson nondiagonal transitions and $\langle g_0|\tilde{H}_2|g_0\rangle = 0$ due to the definition for η in Ref. [44]. The contributions of these nondiagonal terms to the physical quantities are $O(g_k^4)$. For zero temperature, contributions from these multiboson nondiagonal transitions may be neglected safely. Since Shiba's relation and the sum rule for the equilibrium correlation function [52] constitute two important checks, it has been shown that they are exactly satisfied in both the Ohmic and sub-Ohmic cases and also justified in the entire parameter regime from weak coupling to strong coupling [44].

III. COMPARISON BETWEEN T-DMRG AND THE VARIATIONAL THEORY

In the spin-boson model, Δ and α are the two most important parameters with competing influences on the system dynamics: the former permits coherent tunneling between the two energy levels, while the latter acts as a damping mechanism. It was found that the Davydov D_1 ansatz works well within the regime of strong spin-boson coupling (i.e., for large α) [33,34]. However, there exist few discussions on the extent of applicability of this ansatz with small α. Fortunately, t-DMRG is rather accurate in this regime, as the phonon excitations are not abundant and the truncation of the Hilbert space will not lead to a precision breakdown. Hence, the t-DMRG results in this parameter regime are able to serve as a comparison to check the accuracy of this ansatz.

Figure 1 compares results from the t-DMRG calculations and the D_1 ansatz in the absence of the magnetic field, i.e., with zero bias ($\epsilon = 0$). It is interesting to examine the time evolution of the up-state population ρ_+, which is set to unity at $t = 0$. In each panel, results are shown for three values of Δ, i.e., $\Delta = 0.02, 0.05$, and 0.1. For small values of α in the range between 0.01 and 0.02, good agreement is found between results from the two approaches even if Δ varies by a large extent. A transition of the population evolution from incoherent to coherent regime can be clearly observed with increasing tunneling constant Δ. With an increase in α, the results from the two approaches start to deviate from each other. In t-DMRG, the coherent oscillation survives for large values of α, while in the result obtained with the Dirac-Frenkel variation using the D_1 ansatz, the oscillation is damped very quickly. Such comparisons are useful to map out the validity ranges of the two approaches. In particular, the good agreement in the weak-coupling regime may point to a reliable application of the Davydov D_1 ansatz to a parameter regime not previously known to be applicable to.

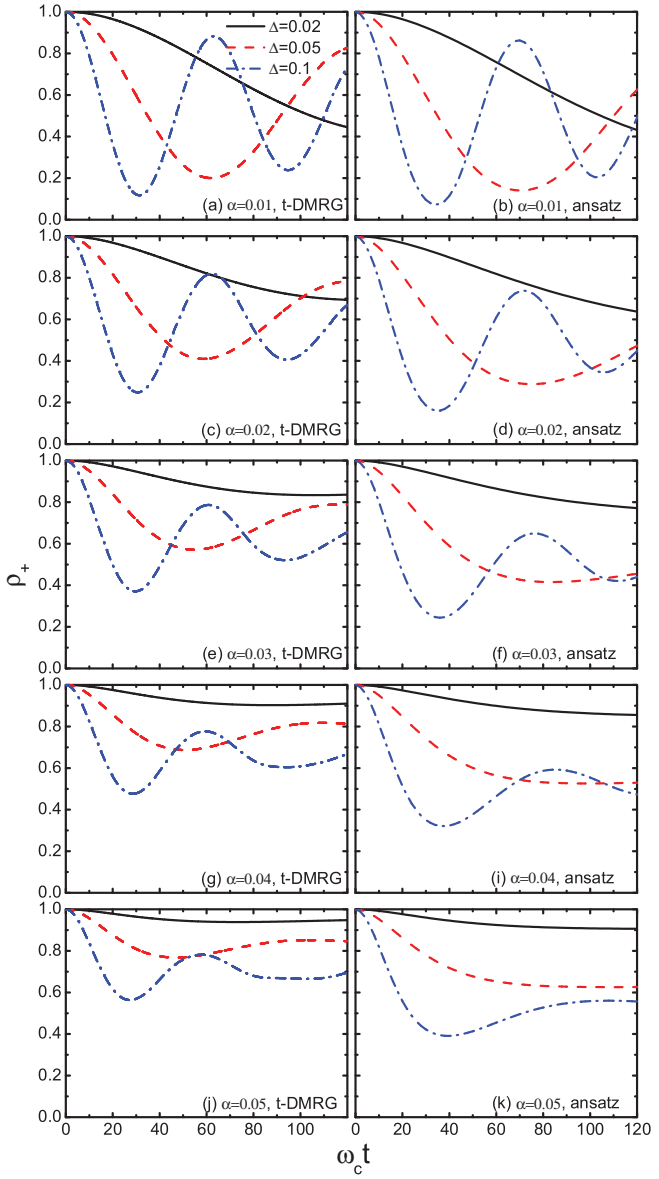

FIG. 1. (Color online) Time evolution of the up-state population for $\epsilon = 0$ and $\Delta = 0.02$ (solid black), 0.05 (dashed red), and 0.1 (dash-dot blue). The left panels are from t-DMRG, and the right panels are from the D_1 ansatz.

Note that there is a small difference in both the amplitude and frequency of the population oscillation between the results of the two methods, due to the fact that, in the t-DMRG approach, it is hard to establish a rigorous spin-up state as the initial state. While in the D_1 ansatz, under the factorized initial condition, the bosonic bath is initially in the vacuum state, and if the polarized initial state is referred to, the bath is initially in a coherent state. To study the influence of the initial state, the population evolution, calculated from the D_1 ansatz, is compared for the factorized and polarized initial states in Fig. 2. It is shown that there is only a modest difference in both the amplitude and the frequency of the up-state population.

In order to see more clearly the origin of the deviation in strong coupling, we show the evolution of $\xi \equiv \langle \hat{b}^\dagger + \hat{b} \rangle / 2$ for several boson sites that are close to the spin with fixed

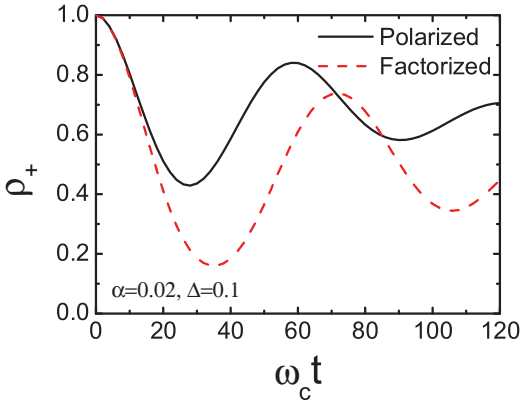

FIG. 2. (Color online) Time evolution of the up-state population calculated by the variational theory using the D_1 ansatz for both the polarized (solid black) and factorized (dashed red) initial conditions when $\alpha = 0.02$ and $\Delta = 0.1$.

$\Delta = 0.05$ in Fig. 3. The value of ξ is proportional to the boson displacement, and, therefore, to the variational parameters $B_{n,l}$ in the Davydov D_1 ansatz, so it is a convenient indicator for possible breakdowns of our numerical approaches. From the time evolution in Fig. 3, it is found that, following time evolution, bosons in an increasing number of sites are excited gradually, and, more importantly, the displacements of the first five sites at least are along the same orientation. This means the boson sites are moving collectively with acoustic wave modes. These modes exist mainly in the weak-coupling (thus low frequency) regime and, thus, stand for the reason of breakdown in strong-coupling regime for t-DMRG. This can be further clarified by Fig. 3(d) which displays evolution of ξ for the strong-coupling case with $\alpha = 0.1$. It is obvious that in this case there is almost no movement of bosons. We thus conclude that, at the present stage, the t-DMRG method is deficient to study the proper physics of the spin-boson model in the strong-coupling regime.

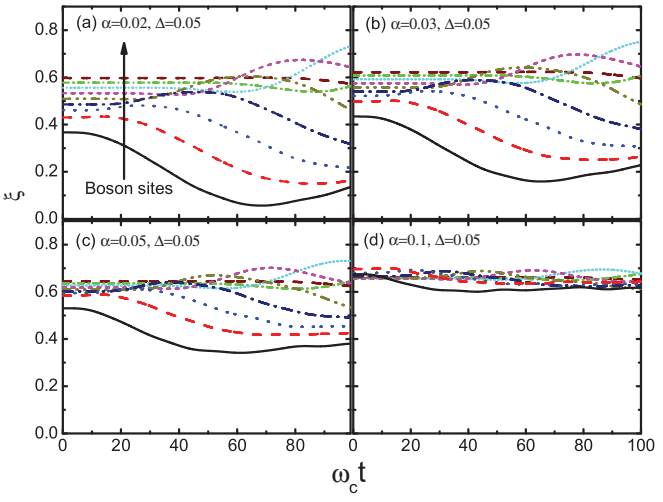

FIG. 3. (Color online) Time evolution of ξ on several boson sites close to the spin for $\Delta = 0.05$, and (a) $\alpha = 0.02$, (b) $\alpha = 0.03$, (c) $\alpha = 0.05$, and (d) $\alpha = 0.1$. The arrow indicates the direction of site index increasing.

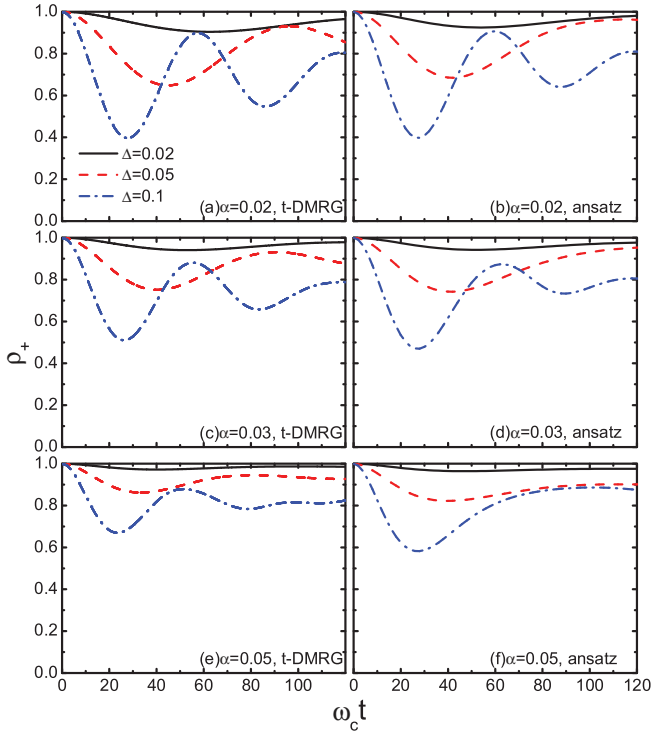

FIG. 4. (Color online) Time evolution of the up-state population for $\epsilon = -0.05$ and $\Delta = 0.02$ (solid black), 0.05 (dashed red), and 0.1 (dash-dot blue). The left panels are from t-DMRG, and the right panels are from the ansatz.

Next, we study the population evolution in the presence of a local field, as shown in Fig. 4. We set ϵ to be -0.05 and focus on the up-state population. The local field introduces an energetic bias for the spin, which is encouraging as the t-DMRG method is known to be more accurate for a gapped system. This is because in a gapped system the high-energy states (above the gap) have vanishingly small contributions to the reduced density matrices, and, as a result, the truncation of states in the DMRG procedure becomes more efficient than in a gapless system. We thus expect that the results of t-DMRG and Davydov D_1 ansatz can be more consistent than the case without bias. Especially for $\alpha = 0.02$ and for $\omega_c t$ shorter than 100, both the approaches yield nearly identical results. However, the t-DMRG method cannot handle well the damping effect at large α over long-time evolution. Based on these results, we conclude that the optimality condition to get reliable results for the t-DMRG method is $\alpha < 0.03$.

In order to quantify the accuracy of the $|D_1\rangle$ ansatz, and to gauge how faithfully $|D_1\rangle$ follows the Schrödinger equation, we define a measure by the name of relative derivation [48], which can be written as

$$\sigma(t) = \frac{\sqrt{\langle\delta(t)|\delta(t)\rangle}}{\bar{E}_{\rm bath}}, \tag{20}$$

where $|\delta(t)\rangle$ is the deviation vector defined in Eq. (3) and $\bar{E}_{\rm bath}$ is the average energy of the bosonic bath which usually corresponds to the largest energy scale in the system. Computed relative deviation curves are displayed in Fig. 5, in which it is demonstrated that the Davydov D_1 ansatz has

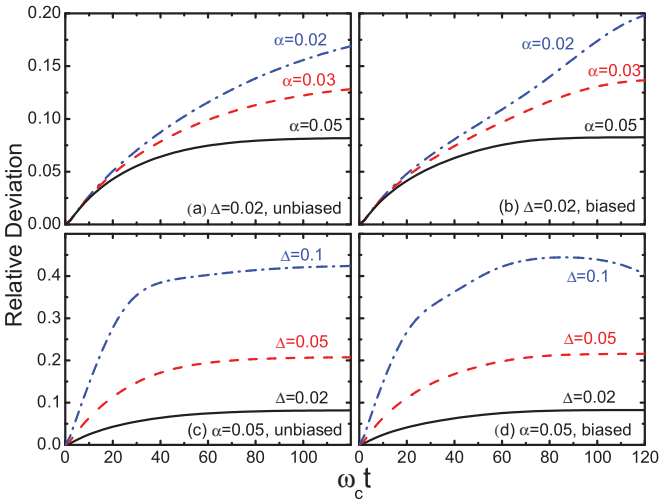

FIG. 5. (Color online) Time evolution of the relative deviation σ, as defined in Eq. (20), for both unbiased and biased ($\epsilon = 0.05$) cases: (a) $\Delta = 0.02$, unbiased; (b) $\Delta = 0.02$, biased; (c) $\alpha = 0.05$, unbiased; (d) $\alpha = 0.05$, biased.

smaller relative deviations when α is large and Δ is small and is, therefore, a good trial state in the strong-coupling regime with or without the bias.

From the aforementioned dynamics computed by the Davydov D_1 ansatz and the t-DMRG method, their validity regimes can be mapped out approximately. The t-DMRG results are reliable in the weak-coupling regime, where the phonon excitations are modest and fall within the acceptable range of the truncated Hilbert space. In the strong-coupling regime, however, the abundant phonon excitations can be hardly described by the truncated Hilbert space, and the bosonic displacement ξ also shows the deficiencies of t-DMRG. Results calculated by use of the Davydov D_1 ansatz are consistent with those from t-DMRG in the weak-coupling regime, inferring that the Davydov D_1 ansatz is sufficiently accurate for weak coupling as well. The validity of the Davydov D_1 ansatz in the strong-coupling regime has been examined in Ref. [48] and also confirmed by the relative derivation calculated in this paper.

Before we move on to the next section, two comments are due. First, despite its high precision in the sub-Ohmic regime, the D_1 ansatz is quite efficient numerically, which allows wide-ranged applications of the trial state to various systems of interest. For the t-DMRG approach, however, computational cost poses the greatest obstacle to extending its applications beyond the spin-boson model as more than 100 hours of CPU time on a single 2.13-GHz processor are needed for each run in this work to achieve adequate accuracies. This hinders possible extensions of the approach to models with many exciton sites, such as the one-dimensional Holstein Hamiltonian. Second, we have also examined the s dependence of the calculation results from the two methods finding that the D_1 ansatz loses accuracy as s is increased, while for t-DMRG, the precision remains on a moderate level. Actually, it is an advantage of t-DMRG to deal with different bosonic baths, such as Ohmic and super-Ohmic baths [41,42].

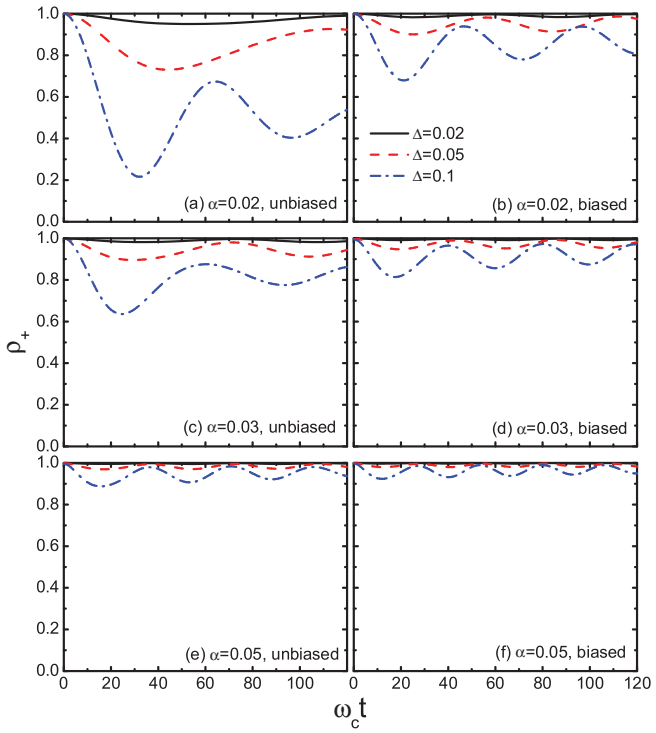

FIG. 6. (Color online) Time evolution of up-state population for both unbiased (left panels) and biased $\epsilon = 0.05$ (right panels) from the perturbative approach with unitary transformation.

IV. NONEQUILIBRIUM TIME EVOLUTION WITH A PERTURBATIVE APPROACH

In this section, a perturbative approach based on a unitary transformation will be used to study the sub-Ohmic spin-boson model in order to provide additional evidence to the validity of the two approaches employed so far. The time evolution of population ρ_+ from the perturbative approach is shown in Fig. 6, in which the left panels show the unbiased non-Markovian dynamics with a sub-Ohmic bath $s = 0.25$ from weak coupling to strong coupling. For large Δ and small α, the dynamics exhibits a coherent underdamped oscillation with a frequency near Δ, which agrees with those of the Davydov D_1 ansatz and t-DMRG. When the coupling strength is large enough, the system is much more localized, and the population dynamics at strong coupling still shows coherent properties with an increasing oscillating frequency. The behavior that the oscillation frequency increases with increases coupling agrees well with that of the PIMC calculations and the analysis of the noninteracting blip approximation [17]. The coherent oscillation survives even for large coupling $\alpha = 0.05$ and the oscillating frequency in $\rho_+(t)$ is much larger than that of t-DMRG and D_1 ansatz. It is worth noting that, in this approach, two approximations have been made: One is the omission of $\tilde{H}_2$ and the other is the usual Born approximation for deriving the master equation. Hence, the validity of our perturbative approach could be lost in some parameter regimes judging from the comparison with the two earlier methods. This comparison, on the other hand, gives a good criterion for evaluating the reliability of the perturbative approach. Besides, the two important checks have been carried out, and the sum rule $\rho_+(t = 0) = 1$ and Shiba's relation have been shown to be satisfied for all the calculated cases.

In addition, we also show, in the right panels of Fig. 6, the biased nonequilibrium population $\rho_+(t)$ for different values of Δ and α. One can see that, apart from the effect of the bias on the long-time population behavior ($\rho_+(t \to \infty)$), a nonzero bias enhances the quantum coherence as the decay rate of the Rabi oscillation for the case of $\epsilon/\omega_c = 0.05$ is lower than that of $\epsilon = 0$. Comparing the biased nonequilibrium population $\rho_+(t)$ for different coupling strengths (under a nonzero bias $\epsilon/\omega_c = 0.05$) with that of the unbiased case, we find that for weak coupling $\alpha = 0.02$, the quantum coherence in the biased case may be kept for a longer time; for the moderate coupling case of $\alpha = 0.05$, the frequency of the biased Rabi oscillation is larger than that of the zero bias case.

V. ENTANGLEMENT DYNAMICS OF TWO QUBITS

In this section, we study first the population transfer process in a spin dimer using the t-DMRG method which has been shown to yield accurate results in the weak-coupling regime. Each of the two spins in the dimer is coupled to an independent bath with a coupling strength of $\alpha = 0.02$, a setup similar to one that has been previously investigated with a focus on persistent electronic coherence [22]. Surprisingly, despite that environment-induced phenomena have been vigorously studied in the field of quantum information processing, scant attention has been paid to entanglement dynamics in Hamiltonians that are composed of spin-boson models [53]. In this work, we aim to study features of entanglement dynamics, such as entanglement sudden death and revival, in a spin dimer with each monomer a two-level system. The Hamiltonian for the spin part has been given in (15).

The initial state to be employed will slightly differ from those used earlier, and on site 1, a local field $\epsilon_1 = -0.2$ will be added initially in the calculation of the ground state and switched off gradually, while on site 2, no such local field is added initially. Therefore, the spin on site 1 is initially in the up state, while site 2 is prepared in a way that depends on the parameters used.

Δ is assumed to be the same for both spins. In Fig. 7, the population and correlation dynamics is displayed for four sets of J and Δ. First, from Figs. 7(a)–7(d), the time-averaged spin-up population on site 1 shows a gradual decrease following an increase in both J and Δ from those in Figs. 7(a) to 7(d), while the spin-up population on site 2 exhibits a tendency to increase gradually. Important difference can be noted between Figs. 7(b) and 7(c). In Fig. 7(b), as J is much smaller than Δ, the spin flipping process dominates. The spin-up populations on sites 1 and 2 are found to share a similar time dependency, pointing to the fact that the increase of the spin-up population on one site comes at the expense of the spin-down population on the same site. On the other hand, in Fig. 7(c), J is much larger than Δ, and the hopping process between the two sites is dominant. We thus can find in this case that the increase of the spin-up population on site 2 is at the expense of that on site 1. In Fig. 7(d), a combined behavior of both flipping and hopping is observed. The results obtained here are in qualitative agreement with those calculated variationally [22]. It is worth noting that when the two parameters J and Δ are

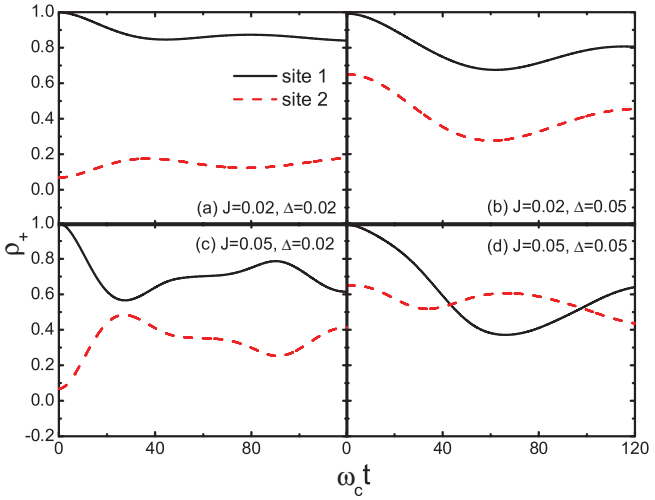

FIG. 7. (Color online) Time evolution of the populations of the spin up state on site 1 (solid black) and site 2 (dashed red) for four sets of control parameters: (a) $J = 0.02$, $\Delta = 0.02$; (b) $J = 0.02$, $\Delta = 0.05$; (c) $J = 0.05$, $\Delta = 0.02$; and (d) $J = 0.05$, $\Delta = 0.05$.

comparable in magnitude, there is an obvious decay in the coherent dynamics. This is nontrivial, since it means the local coherence could be washed out during a nonlocal hopping event, even if there is still a strong local spin flipping rate. We attribute this incoherent transfer to the bath-induced quenching of local spin interference.

To gain further insights, we study the dynamics of entanglement between the two qubits. Concurrence is a well-known measure for the bipartite entanglement given by [54]

$$C(\rho) = \max\{0, \lambda_1 - \lambda_2 - \lambda_3 - \lambda_4\}, \tag{21}$$

with λ_i being the eigenvalues, in decreasing order, of the matrix $\sqrt{\sqrt{\rho}\tilde{\rho}\sqrt{\rho}}$. Here, ρ is the reduced density matrix for the two qubits, and $\tilde{\rho} \equiv (\sigma_y \otimes \sigma_y)\rho(\sigma_y \otimes \sigma_y)$. $C(\rho)$ falls in the range from 0 to 1. If the two qubits are separable, $C(\rho) = 0$, while $C(\rho) = 1$ if they are completely entangled. Calculated concurrences between two independent SBMs are shown in Fig. 8. The initial state for the two qubits is chosen to be an anti-Bell state, which can be written as $a|+-\rangle + \sqrt{1-a^2}|-+\rangle$, while the bosonic bath is initially in the vacuum state. We choose $a = 1/\sqrt{2}$ in our calculation which corresponds to a maximally entangled initial state. Neither the rotating wave approximation nor the Markovian assumption is taken in arriving at the results displayed in Fig. 8, which shows the occurrence of entanglement sudden death at various times [7,14,53,55]. Overall the concurrence lifetime decreases with an increase of the coupling strength.

In Fig. 9, we display the time evolution of the interspin concurrence. The upper panel shows results for the same parameters as those used in Fig. 7 to facilitate easier comparisons. It is not surprising that a large Δ leads to extremely weak entanglement while a large J yields strong entanglement, consistent with earlier discussion. There are two interesting features: (1) the concurrence increases continuously after an initial dip at approximately $\omega_c t = 25$ if both J and Δ are 0.05 and (2) if $J = 0.02$ and $\Delta = 0.05$, the interspin concurrence reemerges after a time period of vanishing entanglement. The latter reproduces the so-called entanglement sudden death and

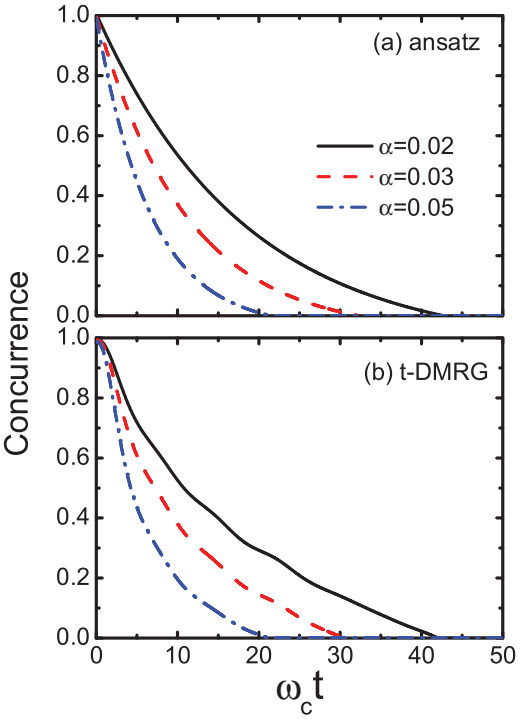

FIG. 8. (Color online) Time evolution of the interspin concurrence calculated by (a) D_1 ansatz and (b) t-DMRG for $\Delta = 0.02$ and $\alpha = 0.02$ (solid black), 0.03 (dashed red), and 0.05 (dash-dot blue).

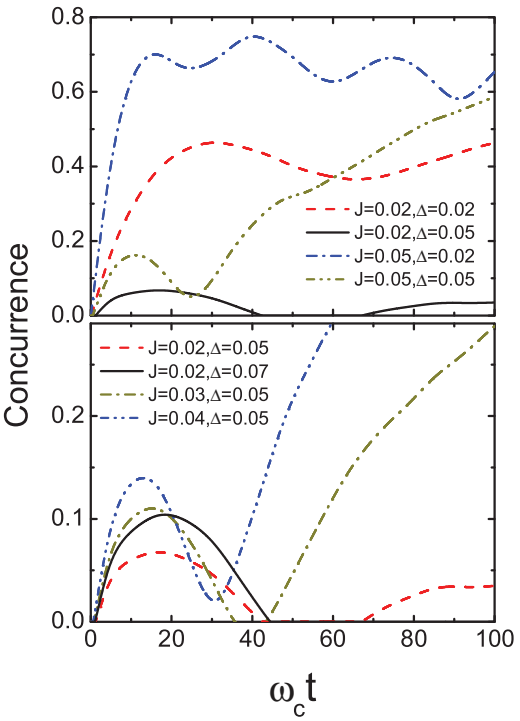

FIG. 9. (Color online) Time evolution of the interspin concurrence for various parameter sets. The parameter sets in the upper panel are the same as those used in Fig. 7. Three additional parameter sets are used in the lower panel with the curve for $J = 0.02, \Delta = 0.05$ replotted for comparison. If Δ is larger than 0.07, entanglement that undergoes a sudden death is not revived, and there is no ESD when J is larger than 0.04.

revival phenomenon [7], an important phenomenon in quantum information processing that has been extensively studied in various systems except in the context of the spin-boson models [53]. In order to determine a parameter range where the entanglement sudden death and revival exist, we display in the lower panel of Fig. 9 the time evolution of the concurrence for three additional sets of parameters. It is found that if $J < 0.03$ and $\Delta > 0.05$, the entanglement sudden death and revival occur after an initial concurrence oscillation. Meanwhile, $\Delta = 0.05$ is the optimal value for such a revival, and for $\Delta = 0.07$, the entanglement will be completely quenched. Further efforts are needed to determine the parameter space for entanglement death and revival. It is worth noting that, while our result is encouraging, we refrain from ascribing it undue importance as the approach taken has insufficient accuracies in the strong-coupling regime. For a careful scrutiny of this otherwise interesting issue, further efforts are needed to improve the reliability of our numerical approaches. In Ref. [55], Wang and Chen employed a hierarchical equation-of-motion approach to study the exact dynamics of quantum correlations of two qubits coupled to bosonic baths. The counter-rotating-wave term has been emphasized, which could suppress the entanglement, especially in the strong-coupling regime. In this work the counter-rotating-wave term and the interqubit interaction are both included.

VI. CONCLUSIONS

We have applied the t-DMRG method with orthogonal polynomial representation and the Davydov D_1 variational ansatz to study the dynamics of the sub-Ohmic spin-boson model. Evolution of the population of the spin-up state as well as the coherence between the up and down states is studied by both approaches with and without a local field. Excellent agreement between the results from the two approaches has been found when the coupling strength is not too large. A third approach, the perturbative approach based on a unitary transformation, is also utilized to help compare the relative accuracy of the two methods. Specifically, the t-DMRG method yields reliable results in the weak-coupling regime; however, in the strong-coupling regime, more phonon excitations emerge which can be poorly described by the truncated Hilbert space. The Davydov D_1 ansatz is supported by the t-DMRG method in the weak-coupling regime, and its validity in the strong-coupling regime has been confirmed by monitoring and making sure the relative deviation remains small. The third perturbative approach based on the unitary transformation generates results at variance with those from the former two methods in the strong-coupling regime, which may result from the Born approximation used in the derivation of the master equation and neglecting higher-order terms in the transformed Hamiltonian. In conclusion, the Davydov D_1 ansatz can deal with both the strong- and weak-coupling regimes with high efficiency and sufficient precision, while the t-DMRG approach is shown to be accurate in the weak-coupling regime and can be used as a method of corroboration in the dynamics calculations.

Using the t-DMRG method and the Davydov D_1 ansatz, we also studied bipartite entanglement dynamics between two qubits coupled with individual bosonic baths. The competition between the hopping integral J and the flipping rate Δ is first discussed, and a nontrivial decay of the local coherence is uncovered when J and Δ are comparable. Following that, the bipartite entanglement between the two spins is studied by evaluating the concurrence, and the entanglement sudden death and its revival are observed.

ACKNOWLEDGMENTS

This work was supported by the Singapore National Research Foundation through the Competitive Research Programme (CRP) under Project No. NRF-CRP5-2009-04. Y.Y. and C.Q.W. were supported in part by the National Natural Science Foundation of China and the National Basic Research Program of China (Grants No. 2009CB929204 and No. 2012CB921400). Z.G.L. was supported in part by the NSF of China (Grants No. 11174198 and No. 10904091) and the NBRPC (Grant No. 2011CB922202). The authors thank Qinghu Chen, Wei Si, and Ning Wu for useful discussions and Prathamesh Shenai for commenting on the manuscript.

[1] R. Hildner, D. Brinks, and N. F. van Hulst, Nat. Phys. **7**, 172 (2011).
[2] Y. C. Cheng and R. J. Silbey, J. Chem. Phys. **128**, 114713 (2008).
[3] J. Gilmore and R. H. McKenzie, J. Phys. Chem. A **112**, 2162 (2008).
[4] X. Hu, T. Ritz, A. Damjanović, and K. Schulten, J. Phys. Chem. B **101**, 3854 (1997).
[5] B. Lanyon, C. Hempel, D. Nigg, M. Müller, R. Gerritsma, F. Zähringer, P. Schindler, J. T. Barreiro, M. Rambach, G. Kirchmair, M. Hennrich, P. Zoller, R. Blatt, and C. F. Roos, Science **334**, 57 (2011).
[6] Y. Kubo, C. Grezes, A. Dewes, T. Umeda, J. Isoya, H. Sumiya, N. Morishita, H. Abe, S. Onoda, T. Ohshima, V. Jacques, A. Dréau, J.-F. Roch, I. Diniz, A. Auffeves, D. Vion, D. Esteve, and P. Bertet, Phys. Rev. Lett. **107**, 220501 (2011).
[7] T. Yu and J. H. Eberly, Phys. Rev. B **68**, 165322 (2003); Phys. Rev. Lett. **93**, 140404 (2004); **97**, 140403 (2006); Science **323**, 598 (2009).
[8] T. A. Costi and R. H. McKenzie, Phys. Rev. A **68**, 034301 (2003); D. V. Khveshchenko, Phys. Rev. B **69**, 153311 (2004).
[9] K. Le Hur, P. Doucet-Beaupré, and W. Hofstetter, Phys. Rev. Lett. **99**, 126801 (2007).
[10] J.-D. Picon, M. N. Bussac, and L. Zuppiroli, Phys. Rev. B **75**, 235106 (2007); Y. Yao, W. Si, X. Y. Hou, and C. Q. Wu, J. Chem. Phys. **136**, 234106 (2012), and references therein.
[11] G. S. Engel, T. R. Calhoun, E. L. Read, T. K. Ahn, T. Mancal, Y. C. Cheng, R. E. Blankenship, and G. R. Fleming, Nature **446**, 782 (2007).
[12] I. P. Mercer, Y. C. El-Taha, N. Kajumba, J. P. Marangos, J. W. G. Tisch, M. Gabrielsen, R. J. Cogdell, E. Springate, and E. Turcu, Phys. Rev. Lett. **102**, 057402 (2009).

[13] A. Troisi and G. Orlandi, Phys. Rev. Lett. **96**, 086601 (2006).
[14] Y. Zhao and G. Chen, Physica A **317**, 13 (2002).
[15] A. J. Leggett, S. Chakravarty, A. T. Dorsey, P. A. Fisher, and A. Garg, Rev. Mod. Phys. **59**, 1 (1987).
[16] U. Weiss, *Quantum Dissipative Systems*, 3rd ed. (World Scientific, Singapore, 2007).
[17] D. Kast and J. Ankerhold, Phys. Rev. Lett. **110**, 010402 (2013).
[18] R. Egger and C. H. Mak, Phys. Rev. B **50**, 15210 (1994); L. Muhlbacher and J. Ankerhold, J. Chem. Phys. **122**, 184715 (2005); L. Muhlbacher, J. Ankerhold, and A. Komnik, Phys. Rev. Lett. **95**, 220404 (2005).
[19] H. Wang and M. Thoss, New J. Phys. **10**, 115005 (2008); Chem. Phys. **370**, 78 (2010).
[20] Z. Lü and H. Zheng, J. Chem. Phys. **136**, 121103 (2012).
[21] A. Ishizaki and G. R. Fleming, J. Chem. Phys. **130**, 234111 (2009).
[22] H. Hossein-Nejad and G. D. Scholes, New J. Phys. **12**, 065045 (2010).
[23] D. P. S. McCutcheon and A. Nazir, Phys. Rev. B **83**, 165101 (2011).
[24] A. W. Chin, J. Prior, S. F. Huelga, and M. B. Plenio, Phys. Rev. Lett. **107**, 160601 (2011).
[25] Y. Y. Zhang, Q. H. Chen, and K. L. Wang, Phys. Rev. B **81**, 121105(R) (2010).
[26] P. Nalbach and M. Thorwart, Phys. Rev. B **81**, 054308 (2010).
[27] N. Makri and D. E. Makarov, J. Chem. Phys. **102**, 4600 (1995); **102**, 4611 (1995); N. Makri, J. Math. Phys. **36**, 2430 (1995); M. Thorwart, P. Reimann, P. Jung, and R. F. Fox, Chem. Phys. **235**, 61 (1998); M. Thorwart, P. Reimann, and P. Hanggi, Phys. Rev. E **62**, 5808 (2000).
[28] A. Winter, H. Rieger, M. Vojta, and R. Bulla, Phys. Rev. Lett. **102**, 030601 (2009).
[29] K. G. Wilson, Rev. Mod. Phys. **47**, 773 (1975).
[30] R. Bulla, N.-H. Tong, and M. Vojta, Phys. Rev. Lett. **91**, 170601 (2003); M. Vojta, N.-H. Tong, and R. Bulla, *ibid.* **94**, 070604 (2005); F. B. Anders, R. Bulla, and M. Vojta, *ibid.* **98**, 210402 (2007).
[31] A. Alvermann and H. Fehske, Phys. Rev. Lett. **102**, 150601 (2009).
[32] T. Holstein, Ann. Phys. **8**, 325 (1959); **8**, 343 (1959).
[33] Y. Zhao, D. W. Brown, and K. Lindenberg, J. Chem. Phys. **106**, 2728 (1997); **106**, 5622 (1997); **107**, 3179 (1997).
[34] Y. Zhao, P. Zanardi, and G. H. Chen, Phys. Rev. B **70**, 195113 (2004); J. Sun, Y. Zhao, and W. Z. Liang, *ibid.* **79**, 155112 (2009).
[35] A. Scott, Phys. Rep. **217**, 1 (1992); A. S. Davydov, Zh. Eksp. Teor. Fiz. **78**, 789 (1980) [Sov. Phys. JETP **51**, 397 (1980)].
[36] Y. Zhao, S. Yokojima, and G. Chen, J. Chem. Phys. **113**, 4016 (2000).
[37] R. Bulla, H. J. Lee, N. H. Tong, and M. Vojta, Phys. Rev. B **71**, 045122 (2005).
[38] S. R. White, Phys. Rev. B **48**, 10345 (1993).
[39] A. W. Chin, Á. Rivas, S. F. Huelga, and M. B. Plenio, J. Math. Phys. **51**, 092109 (2010).
[40] A. J. Daley, C. Kollath, U. Schollwöck, and G. Vidal, J. Stat. Mech.: Theor. Exp. (2004) P04005; S. R. White and A. E. Feiguin, Phys. Rev. Lett. **93**, 076401 (2004).
[41] J. Prior, A. W. Chin, S. F. Huelga, and M. B. Plenio, Phys. Rev. Lett. **105**, 050404 (2010).
[42] C. Guo, A. Weichselbaum, S. Kehrein, T. Xiang, and J. von Delft, Phys. Rev. B **79**, 115137 (2009).
[43] W. Zwerger, Z. Phys. B **53**, 53 (1983); **54**, 87 (1983); H. Dekker, Phys. Rev. A **35**, 1436 (1987); C. Aslangul, N. Pottier, and D. Saint-James, Physica A **149**, 535 (1988).
[44] Z. G. Lü and H. Zheng, Phys. Rev. B **75**, 054302 (2007); C. Zhao, Z. G. Lü, and H. Zheng, Phys. Rev. E **84**, 011114 (2011); H. Zheng and Z. G. Lü, J. Chem. Phys. **138**, 174117 (2013).
[45] M. J. Škrinjar, D. V. Kapor, and S. D. Stojanović, Phys. Rev. A **38**, 6402 (1988).
[46] P. A. M. Dirac, Math. Proc. Cambridge Philos. Soc. **26**, 376 (1930)
[47] J. Frenkel, *Wave Mechanics* (Oxford University Press, Oxford, 1934).
[48] N. Wu, L. Duan, X. Li, and Y. Zhao, J. Chem. Phys. **138**, 084111 (2013).
[49] B. Luo, J. Ye, and Y. Zhao, Phys. Phys. Status Solidi C **8**, 70 (2011).
[50] B. Luo, J. Ye, C. B. Guan, and Y. Zhao, Phys. Chem. Chem. Phys. **12**, 15073 (2010).
[51] R. Silbey and R. A. Harris, J. Chem. Phys. **80**, 2615 (1984).
[52] T. Stauber, Phys. Rev. B **68**, 125102 (2003).
[53] C. E. López, G. Romero, F. Lastra, E. Solano, and J. C. Retamal, Phys. Rev. Lett. **101**, 080503 (2008).
[54] W. K. Wootters, Phys. Rev. Lett. **80**, 2245 (1998).
[55] L. W. Duan, H. Wang, Q. H. Chen, and Y. Zhao, J. Chem. Phys. **139**, 044115 (2013); C. Wang and Q. H. Chen, arXiv:1303.1054 [New J. Phys. (to be published)].